



AIAA-2002-3815

**Pressure Map of a Facility as a
Function of Flow Rate to
Study Facility Effects**

Mitchell L. R. Walker, Alec D. Gallimore
Plasmadynamics and Electric Propulsion Laboratory
The University of Michigan
Ann Arbor, MI 48105 USA

Chunpei Cai, and Iain D. Boyd,
Nonequilibrium Gas and Plasmadynamics Group
The University of Michigan
Ann Arbor, MI 48105 USA

**38th AIAA/ASME/SAE/ASEE
Joint Propulsion Conference & Exhibit
7-10 July 2002
Indianapolis, Indiana**

For permission to copy or republish, contact the copyright owner named on the first page.
For AIAA-held copy write, write to AIAA Permissions Department,
1801 Alexander Bell Drive, Suite 500, Reston, VA 20191-4344.

PRESSURE MAP OF A FACILITY AS A FUNCTION OF FLOW RATE TO STUDY FACILITY EFFECTS

Mitchell L.R. Walker* Alec D. Gallimore†
mwalker@engin.umich.edu alec.gallimore@umich.edu

Plasmadynamics and Electric Propulsion Laboratory
Department of Aerospace Engineering

Chunpei Cai* Iain D. Boyd‡
ccai@engin.umich.edu iainboyd@umich.edu
Nonequilibrium Gas and Plasmadynamics Group

University of Michigan
Ann Arbor, MI 48109 USA

ABSTRACT

A neutral gas background pressure map of the Large Vacuum Test Facility (LVTF) at the University of Michigan is presented. The LVTF was mapped at a series of cold anode flow rates corresponding to P5 Hall thruster operating conditions of 1.5, 3.0, and 9.0 kW. The chamber pressure was mapped at nominal xenon pumping speeds of 140,000 and 240,000 l/s with a rake consisting of five calibrated Bayard-Alpert (BA) hot-cathode ionization gauges. The cold flow results were used to validate a full 3-D numerical model of the LVTF with a cold-flowing Hall thruster. This computational facility model was built with MONACO, a 3D unstructured direct simulation Monte Carlo method (DSMC) code that includes asymmetric features such as the gridded chamber floor and cryopumps. This investigation is intended to begin initial development of the facility effects characterization being pursued by the Plasmadynamics and Electric Propulsion Laboratory (PEPL) at the University of Michigan. The measured axial pressure profiles on the thruster centerline indicate that the plume expands to the facility background pressure in approximately 1.7 m. The plume expansion appears to be independent of anode flowrate and facility background pressure. The experimental and computational data exhibit the same general trends. However, there is a discrepancy of a factor ranging between 4 and 6 between the measured data and the computed results. This discrepancy is thought to stem from the choice of neutral-to-cryosurface sticking coefficient and a high computational cryosurface temperature. The next steps include modifying the model, making a similar cold-flow map of a NASA vacuum facility, and making a hot-flow map of the LVTF.

* Graduate Student, Student Member AIAA

† Associate Professor, Associate Fellow AIAA

‡ Associate Professor, Senior Member AIAA

Introduction

It is technically challenging and expensive to create the on-orbit environment in a ground-based laboratory facility. All ground-based vacuum facilities possess a low-density background neutral gas due to physical pumping limitations and the leak rate of the facility. As gas is introduced into the vacuum chamber in the form of propellant, the background pressure rises until the pumping speed, facility leak rate, and propellant flowrate equilibrate for the operating condition. The facility background gas present in the vacuum chamber can distort the exhaust plume of the thruster.¹ High-energy exhaust particles interact with the neutral background particles through charge exchange collisions (CEX).² In the plume, the effects of CEX products are most evident in the perimeter, where they lead to an increase in the measured current density. Thruster operation and performance are dependent on the background pressure of the facility.³ At elevated background pressures, residual gas particles can be entrained into the thruster discharge region artificially increasing engine thrust. Elevated facility pressure has also been found to increase the width of the ion energy distribution function through elastic collisions between beam ions and neutral background particles.⁴ Due to these effects, the validity of comparisons made between data taken in facilities with different background pressures, especially at 10^{-4} Torr and higher, is questionable. However, comparisons have been made between data taken in Russia and NASA.⁵ In order to correlate data taken in ground based facilities to in-space thruster performance, the effect of facility background pressure on thruster operation must be fully characterized and taken into account when analyzing test data. Because of the drastic implications of facility effects, electric propulsion technology has reached the point where standard guidelines must be developed for test facilities to ensure reliable engine development and testing.⁵ This need has become even more pressing now that 50+ kW Hall thrusters are being developed.⁶

Several investigations are underway to numerically model thruster performance and the interactions between Hall thrusters and spacecraft.^{7,8} The results of these models are highly dependent on experimentally measured boundary conditions. One of the most important auxiliary inputs required by these codes is background pressure of a laboratory vacuum chamber.⁷

The University of Michigan's Plasmadynamics and Electric Propulsion Laboratory (PEPL) has launched an investigation of facility effects introduced by elevated backpressures. This investigation has thus far included

measuring the performance of the P5 HET at different pumping speeds,⁹ an evaluation of a collimated Faraday probe's ability to filter out CEX ions while measuring the ion current density at elevated back pressures,^{2,10} and a comparison of NASA Glenn Research Center's (GRC) and Jet Propulsion Laboratory's (JPL) nude Faraday probes.¹¹

The objective of the experiment presented in this paper is to create a pressure map of the LVTF at a series of cold[§] anode flow rates corresponding to typical P5 Hall thruster operating conditions at different facility pumping speeds. This is the first step in creating a technique for making neutral density pressure maps with hot flow in a Hall thruster facility. The results of the cold flow pressure map were then compared to a numerical simulation of the chamber in order to develop the tools that will be necessary to correct for facility effects.

In the following, we explain the experimental apparatus, present the experimental results, and discuss the experimental and numerical results. Finally, some conclusions and directions for future work are offered.

Experimental Apparatus

Vacuum Facility

All experiments were conducted in the University of Michigan's Large Vacuum Test Facility (LVTF). The NASA-173M was mounted at thruster station 1, as indicated in Figure 1. The LVTF is a stainless steel clad vacuum chamber that has a diameter of 6 m and a length of 9 m. Two 2,000 CFM blowers and four 400 CFM mechanical pumps evacuate the LVTF to moderate vacuum (30 - 100 mTorr). To reach high vacuum the LVTF is equipped with seven CVI TM-1200 re-entrant cryopumps, each of which is surrounded by a LN₂ baffle. The combined pumping speed of the facility is 500,000 l/s on air, and 240,000 l/s on xenon with a base pressure of 2.5×10^{-7} Torr. The cryopump system can be operated with any number of pumps in use. For the experiments reported here, the LVTF was operated with seven cryopumps. At the average anode flow rates investigated—5.25, 10.46, and 14.09 mg/s, all with a 0.60 mg/s cathode flow—

[§] Throughout the paper, we use the phrase "cold flow" to denote xenon flowing through the thruster anode and cathode without a plasma discharge and "hot flow" to denote xenon flowing through the anode and cathode of a thruster in operation.

and at a nominal xenon pumping speed of 240,000 l/s, the operating pressures of the LVTF were approximately 1.7×10^{-6} , 7.7×10^{-6} , 1.0×10^{-5} Torr on xenon, as shown in Table 1.

Chamber pressure was monitored by two hot-cathode ionization gauges, as indicated in Figure 1. The first gauge was a Varian model Bayard-Alpert (BA) gauge with a HPS model 919 Hot Cathode Controller. The BA model 571 ionization gauge is connected to the chamber via a 25-cm-long, by 3.48-cm-inner-diameter, tube. The second is a Varian model UHV-24 nude gauge with a Varian UHV senTorr Vacuum Gauge Controller. This unit was calibrated on air by the manufacturer. Pressure measurements from both gauges were corrected for xenon using the known base pressure on air and a correction factor of 2.87 for xenon according to the following equation¹²

$$P_c = \frac{P_i - P_b}{2.87} + P_b, \quad (1)$$

where P_c is the corrected pressure on xenon, P_b is the base pressure, and P_i is the indicated pressure when xenon is flowing into the vacuum chamber. The corrected average pressure of the two gauges is normally reported as the chamber background pressure. All pumping speeds and pressures reported in the following are corrected for xenon.

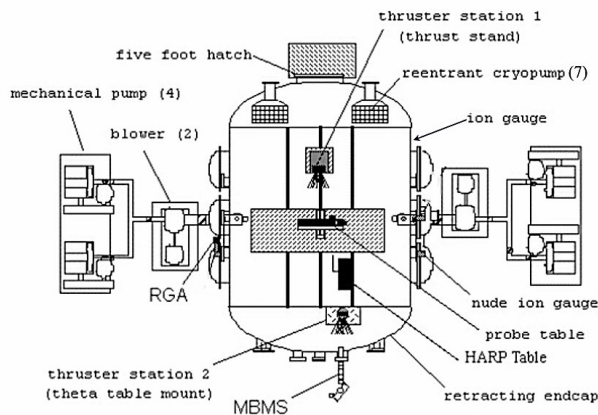


Figure 1 – Schematic of the LVTF.

Hall Thruster

All experiments were performed on the P5-2 (also known as the NASA-173M) 5 kW laboratory-model Hall thruster. A more detailed discussion of this thruster can be found in Ref. 9. This thruster is designed to operate in both single- and two-stage modes. For these experiments, the electrode used for

two-stage operation was replaced with the same ceramic used in the chamber walls, enabling the engine to be operated as a single-stage device. The NASA-173M has a mean diameter of 148 mm, a channel width of 25 mm, and has a nominal power rating of 5 kW.⁹ For these experiments, xenon was flowed through the thruster anode and no plasma discharge was present.

A NASA GRC laboratory-model hollow cathode was located at the 12 o'clock position on the thruster. The cathode orifice was located approximately 25 mm downstream and 25 mm radially away from the outer front pole piece at an inclination of 30° from the thruster centerline. Xenon flow rates corresponding to the necessary flow rates of the operating NASA-173M Hall thruster were set on the cathode. This will yield comparable backpressures for future pressure maps with the NASA-173M Hall thruster operating.

High-purity (99.999% pure) xenon propellant was supplied to the Hall thruster from compressed gas bottles through stainless-steel feed lines. Anode and cathode propellant flows were controlled and monitored with MKS 1179A mass flow controllers. The flow controllers were calibrated with a custom apparatus that measures gas pressure and temperature as a function of time in an evacuated chamber of known volume. The mass flow controllers have an accuracy of $\pm 1\%$ full scale.

Ionization Gauge

The BA hot-cathode ionization gauge accurately measures pressure over the range of 10^{-4} to 10^{-12} Torr.¹⁰ Estimates of the pressure for the experiment were 10^{-5} to 10^{-8} Torr, based on previous experimental data. Because of its accuracy over the anticipated range of pressures, the BA gauge was selected to measure the chamber pressure field.

Five Varian 571 BA type standard range ionization gauge tubes were used to measure the chamber pressure field because of their rugged construction, low cost, and long life. Future work at PEPL will include a hot flow pressure map of the LVTF. Thus, the BA gauges need a neutralizer to ensure that the plasma does not affect pressure measurements, per Varian's recommendation. To make the hot and cold flow experiments identical in setup, the neutralizers were present during the cold flow experiment. The neutralizer design prevents plume ions from having a direct line of sight to the ionization gauge filament. The neutralizer contains two 72 mesh screens (0.5 by 0.5 mm and 1.0-mm-thick) to ensure neutralization of any ions that travel inside the orifice and that are not

neutralized by wall collisions. Figure 2 shows the Varian 571 BA ionization gauge and the neutralizer along with their mounting position with respect to the cold flow direction.

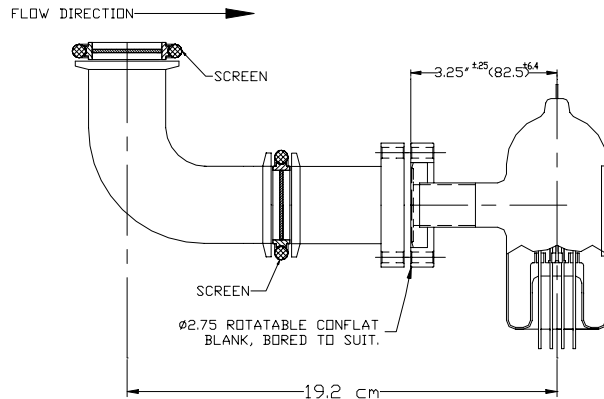


Figure 2 – Schematic of the Varian 571 BA Ionization Gauge connected to the neutralizer.

Two of the BA gauges were controlled by separate Varian senTorr gauge controllers. The remaining three BA gauges were controlled by a Varian Multi-Gauge controller. The Multi-Gauge controller simultaneously controlled each of the three BA gauges and allowed the user to scroll through a display of the pressure for each gauge.

Ionization Gauge Calibration

Calibration of the five ionization gauge systems was performed by the NASA GRC Calibration Laboratory. Each system, comprising of a BA gauge, the actual internal and external cables used in the LVTF mapping, a Varian 10-wire vacuum chamber instrumentation feedthrough, and a Varian BA circuit board mounted in either the senTorr or Multi-Gauge controller, was calibrated with nitrogen as a one-piece unit using a National Institute of Standards and Technology traceable spinning rotor gauge.

Ionization Gauge Positioning System

To generate the two-dimensional mapping inside the vacuum chamber, we mounted the ionization gauges to a custom built, two-axis positioning stage developed by New England Affiliated Technologies (NEAT). The positioning system is composed of a 1.8-m-long linear stage in the radial direction that is mounted on a 0.9-m-long axial stage with an absolute linear position accuracy of 0.15 mm. A LabView VI controlled the motion of the two linear position tables, which in turn moved the Ionization Gauge Positioning System

(IGPS) that carried the five BA gauges used to survey the chamber. Figure 3 shows a schematic of the IGPS mounted within the LVTF. The IGPS allowed the pressure measurements to be taken throughout the majority of the chamber with a single evacuation cycle of the LVTF. The area mapped by the IGPS encompasses an area with a minimum distance from the thruster of 0.5 m, encompassing the typical 1 m distance plume properties are measured.

Figure 4 displays the IGPS mounted in the LVTF and the 25 cm X 25 cm grid on which data points were taken. The solid circles indicate the position of each of the five probes when the IGPS is in the initial position. The note in Figure 4 denotes that gauge 2 is positioned on the opposite side of the chamber centerline to avoid being immersed in any wake effects created by gauge 3. Figure 4 also shows the coordinate system used for this experiment and the numerical simulation. The coordinate system origin is located at the discharge chamber exit plane on the thruster centerline. Where negative X is to the left and positive Y is up.

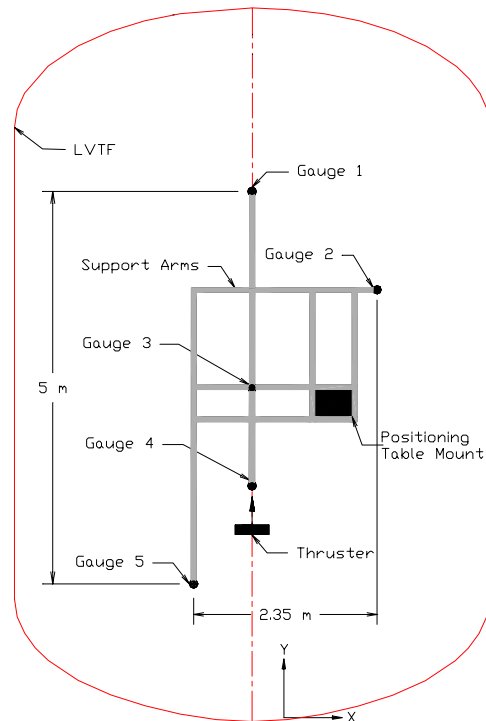


Figure 3 – Schematic of the IGPS mounted in the LVTF.

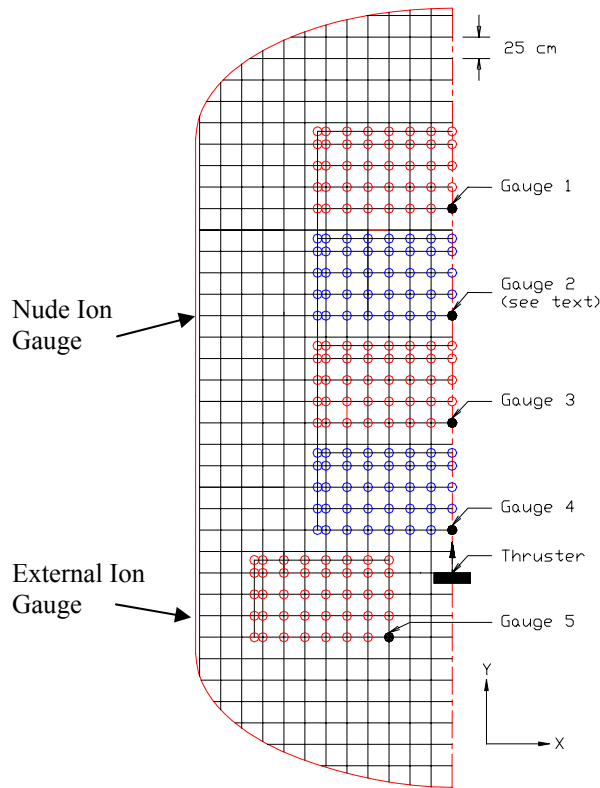


Figure 4 – LVTF half-plane (looking down) with the IGPS and a 25 cm X 25 cm grid. Each open circle denotes the location of a data point.

Experimental Results

To operate the BA gauges on the IGPS, a custom set of cables were constructed. These cables pass through the chamber wall on the five, 10-wire instrumentation feedthroughs. The overall cable lengths from controller to BA gauge were approximately 15 and 23 m, depending on the location of the particular gauge. To verify the operation of each line after the setup was complete, a sealed-glass ionization gauge was operated with a senTorr controller. Varian reports that the reference ionization tube is sealed-off at less than 5.0×10^{-6} Torr. Each of the ionization gauge systems measured pressures below the maximum pressure reported by the vendor. This test confirmed the operation of the equipment while the LVTF was at atmosphere to avoid unnecessary evacuation cycles of the vacuum chamber. The BA gauges mounted to the IGPS measured pressures within a few percent of the pressure reported on the nude ionization gauge. This comparison confirmed that the ionization gauges mounted on the IGPS were operating properly at vacuum.

To determine if the neutralizer conductance significantly reduces the pumping speed to the ionization gauge, which would result in large response times, the anode mass flowrate was increased from 0 to 5 mg/s over a time interval of 10 seconds. The internal ionization gauges displayed response times comparable to the two chamber gauges, which measure the chamber background pressure. Next, the anode mass flowrate was decreased from 5 to 0 mg/s over a 10 second time interval. The internal ionization gauges once again displayed response times comparable to the two chamber gauges. This test gave confidence that the neutralizer did not adversely affect gauge operation.

We assumed that chamber pressure was horizontally symmetric about the chamber centerline. This assumption reduced the number of spatial positions that had to be mapped. All pressure map data presented will only be from one side of the chamber.

Table 1 presents the thruster and chamber operating conditions that were investigated. Table 1 shows the average pressures measured with the nude and external gauges. Initially, the chamber background pressure was mapped with zero propellant flowrate into the chamber to evaluate the chamber background pressure. Then the chamber pressure was mapped at anode flowrates of approximately 5.25, 10.46, and 14.09 mg/s for nominal facility pumping speeds of 140,000 and 240,000 l/s.

Figures 5 - 9 present the pressure map data corrected for xenon. The excluded data showed results consistent with the observations in the figures presented at all cold flowrates.

Table 1 – P5-2 Cold Flow operating conditions.

| Anode Flow (mg/s) | Cathode Flow (mg/s) | Nominal Pumping Speed (l/s) | Average Pressure (Torr-Xe) |
|-------------------|---------------------|-----------------------------|----------------------------|
| 0.00 | 0.00 | 140,000 | 5.3E-07 |
| 5.25 | 0.60 | 140,000 | 7.7E-06 |
| 10.46 | 0.60 | 140,000 | 1.3E-05 |
| 14.09 | 0.60 | 140,000 | 1.7E-05 |
| 0.00 | 0.00 | 240,000 | 3.4E-07 |
| 5.25 | 0.60 | 240,000 | 1.9E-06 |
| 10.46 | 0.60 | 240,000 | 7.9E-06 |
| 14.09 | 0.60 | 240,000 | 1.1E-05 |

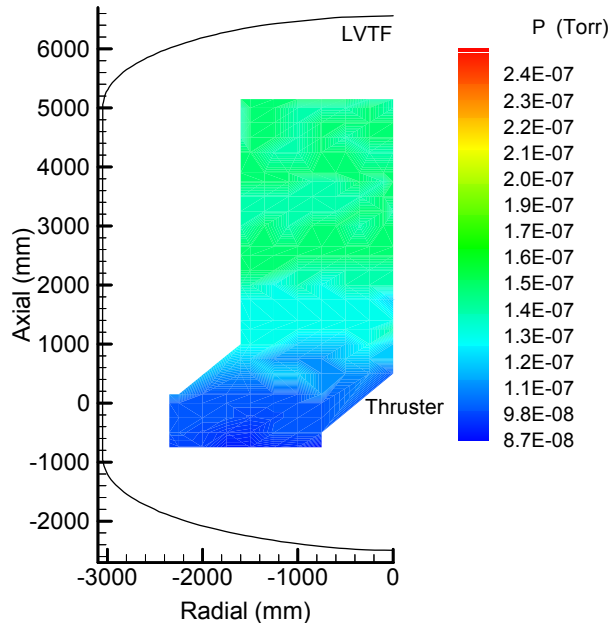


Figure 5 – Pressure Map of the LVTF at a propellant flow rate of 0 mg/s, at a nominal pumping speed of 240,000 l/s. The nude gauge measured 2.5×10^{-7} Torr and the external gauge measured 4.3×10^{-7} Torr.

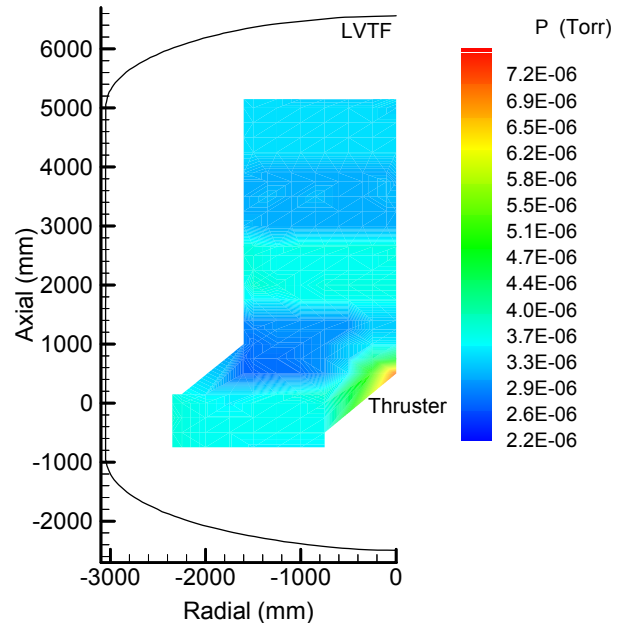


Figure 7 – Pressure map of the LVTF with an anode flow rate of 5.25 mg/s and a cathode flowrate of 0.60 mg/s, at a nominal pumping speed of 140,000 l/s. The nude gauge measured 4.9×10^{-6} Torr and the external gauge measured 9.8×10^{-6} Torr, corrected for xenon.

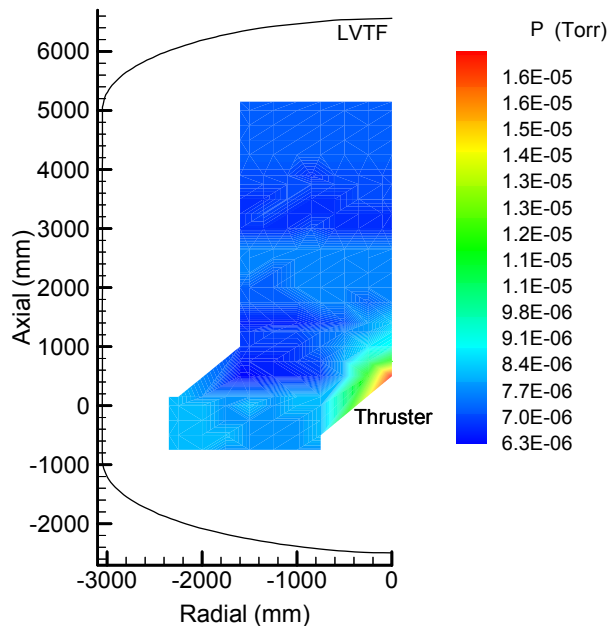


Figure 6 – Pressure Map of the LVTF with an anode flow rate of 14.09 mg/s and a cathode of 0.60 mg/s, at a nominal pumping speed of 240,000 l/s. The nude gauge measured 7.0×10^{-6} Torr and the external gauge measured 1.4×10^{-5} Torr, corrected for xenon.

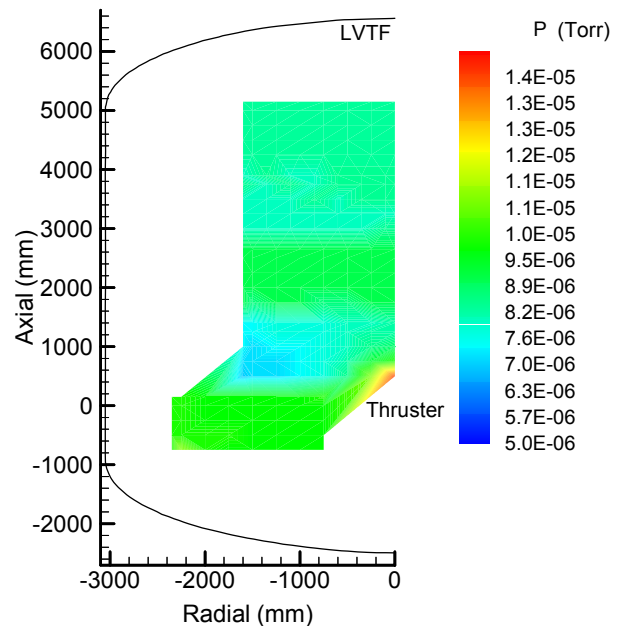


Figure 8 – Pressure map of the LVTF with an anode flow rate of 10.46 mg/s and a cathode of 0.60 mg/s, at a nominal pumping speed of 140,000 l/s. The nude gauge measured 8.4×10^{-6} Torr and the external gauge measured 1.7×10^{-5} Torr, correct for xenon.

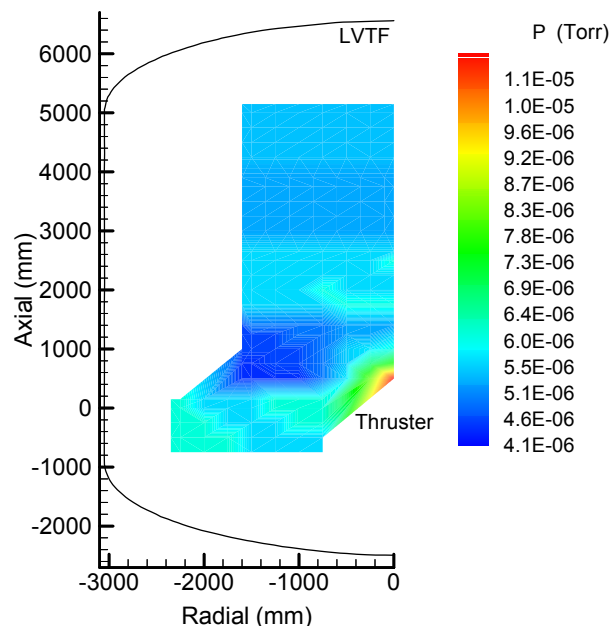


Figure 9 – Pressure map of the LVTF with an anode flow rate of 10.46 mg/s and a cathode flow rate of 0.60 mg/s, at a nominal pumping speed of 240,000 l/s. The nude gauge measured 5.2×10^{-6} Torr and the external gauge measured 1.0×10^{-5} Torr, corrected for xenon.

Discussion

Figure 5 presents the pressure field at a nominal pumping speed of 240,000 l/s with zero propellant entering the chamber. The cryopumps are located on the chamber walls behind station 1 as indicated in Figure 1. The chamber back pressure clearly varies from a minimum just in front of the cryopumps to a maximum at the opposite end of the LVTF.

Figure 5 indicates that a “high” pressure region exists over the axial locations of 3-4 m. The high-pressure region exists over exactly the same area that gauge 2 interrogates, as seen in Figure 2. This is not a coincidence. The ionization gauges were calibrated over the widest range the GRC Calibration Laboratory could accommodate at the time; 5×10^{-5} to 2×10^{-6} Torr. The background pressure for the operation conditions in

Figure 5 is clearly in the low 10^{-7} Torr range. Therefore, it was impossible to make valid corrections to the measured pressures outside of the calibration range. The calibration offset of gauge 2 is merely larger than that of the other gauges and the high-pressure zone is not real. What is important to emphasize is that the pressure over the interrogation area of gauge 2 is nearly constant, which means that

critical details of the pressure field have not been missed due to an inadequate range of calibration. The effect of the limited calibration range is seen to a smaller degree in all of the data taken in this investigation.

Normally, the base pressure of the LVTF is reported as the average of a nude ionization gauge and a glass-covered ionization gauge located at two different axial positions on the chamber, as shown in Figure 1. This method yields a reported base pressure of 3.4×10^{-7} Torr for the conditions in Figure 5. For this condition, 2.5×10^{-7} and 4.3×10^{-7} Torr, were the measured pressures for the nude and external ionization gauges, respectively. The nude gauge reading of 2.5×10^{-7} Torr, is a much better estimate of the true chamber base pressure based on the facility pressure map in Figure 5. This trend holds for all data taken in the experiment. The external ionization gauge is connected to the chamber via a 25 cm long, by 3.48 cm inner diameter, tube. The tube conductance decreases the pumping speed to the ionization gauge, thus yielding unnecessarily high measurements of the chamber pressure.

Figure 6 shows the pressure map of the chamber at a nominal pumping speed of 240,000 l/s with an anode flowrate of 14.09 mg/s. This combination represents the maximum pumping speed and flowrate investigated in this experiment. The chamber background pressure is elevated due to the high anode flowrate, but the plume has expanded to the background pressure at approximately 1.7 m downstream of the anode. Figure 7 and Figure 8 present the pressure maps at a nominal pumping speed of 140,000 l/s for anode flowrates of 5.25 and 10.46 mg/s. Axial pressure profiles on the thruster centerline show that increasing the mass flow rate increases the pressure immediately downstream of the anode. For both flowrates, the plume has expanded to the chamber operating pressure at approximately 1.7 m downstream of the anode. As the flowrate increases, the pressure gradient in the plume increases, but the length of the plume expansion to the chamber background pressure remains constant. This trend was seen for each of the three flowrates.

Figures 8 and 9 present the pressure maps at an anode flowrate of 10.46 mg/s for nominal pumping speeds of 140,000 and 240,000 l/s. The results show that increasing pumping speed only affects the background pressure of the chamber and not the length over which complete plume expansion occurs. However, increasing the pumping speed may become very important when analyzing the hot flow plume expansion, as additional background particles will

increase the number of ions created through CEX collisions.

In addition to mapping the chamber pressure with BA gauges, a numerical simulation was performed. The goal of creating a simulation is to develop a numerical tool to assist in calibrating facilities running at elevated background pressures.

Computational Analysis

Computation of the neutral cold flow of xenon gas from the P5 Hall thruster into the LVTF is performed in three dimensions using the direct simulation Monte Carlo method (DSMC).¹⁶ In the DSMC technique, particles are used to simulate the motions and collisions of real atoms. In the present work, a general 2D/3D implementation of the DSMC method called MONACO¹⁷ is employed. The xenon flow out of the thruster is simulated using a simple source model assuming sonic flow conditions, a temperature of 300 K, and using the measured mass flow rate. The emphasis in the present study is to include as much geometric detail as possible of the LVTF. Thus, an accurate description of the cylindrical chamber is employed, and the seven surfaces of the cryopumps are included in the computational mesh. The three-dimensional unstructured mesh is generated using the Hypermesh software¹⁸ and various views of the mesh are shown in Fig. 10. The mesh contains 11,000 non-uniform cells and 5,000 surface elements. The thruster is located slightly above the vertical center of the chamber and is fired in the direction away from the panels. On the surfaces of the vacuum chamber, fully diffuse reflection is assumed at a wall temperature of 300 K. As discussed by Ketsdever¹⁹, sticking coefficients of common gases with a temperature of 300 K on cryo-panels at a temperature of 15 K range between 0.62 and 0.86. It should be noted that no data appear to exist in the literature specifically for xenon. Any xenon atoms reflecting from the panels are simulated assuming fully diffuse reflection at a temperature of 40 K. In the MONACO computation, momentum exchange collisions between the xenon atoms are simulated using the Variable Hard Sphere (VHS) collision model¹⁶ with the following parameters: $T_{ref}=300$ K, $\omega=0.35$, $d_{ref}=5.31 \times 10^{-10}$ m.

Computational Results

Simulations are performed for the case of a mass flow rate of 10 mg/sec and all 7 cryopumps in operation. Computational results are presented for xenon sticking coefficients of 1.0 (the limiting case of perfect pumping) and 0.85 (the upper bound of values reported

for common gases in Ref. 19). To accelerate convergence, a large time-step is employed in the early stages of each simulation. Steady state is reached after 2,500,000 iterations. Sampling is then performed over a further 50,000 iterations using a time-step of 2×10^{-6} sec. At this point, there are about 250,000 particles in the computational domain.

In Figure 11, contours of pressure predicted by the DSMC computation are shown in the vertical (x-z) plane through the geometric center (y=0) of the chamber. This result is obtained using a value of 0.85 for the sticking coefficient of the cryo-panels. The plot clearly illustrates the location of the thruster above the z=0 center plane of the chamber. The non-symmetric location of the thruster leads to a relative accumulation of pressure along the lower surface of the chamber. The streamlines included in the plot are only suggestive of the flow direction due to the high diffuse and rarefied nature of the gas flow in the chamber. Figure 12 shows the same plot in the horizontal (x-y) plane through the geometric center (z=0) of the chamber. Here again can be seen the relative accumulation of gas in the “corners” of the chamber. Finally, Figure 13 shows the pressure contours computed across the end wall of the chamber located downstream of the thruster. Once again, the build-up of gas in the corners and along the lower surface of the chamber is clearly illustrated.

In Figure 14, direct comparison is made of the pressure in the x-direction along the centerline of the chamber between the experimental measurements and the two computational results using sticking coefficients of 1.0 and 0.85. As expected, the use of the lower sticking coefficient leads to an increase in chamber pressure. Although the experimental and computational data exhibit the same general trends, there is a discrepancy of a factor ranging between 4 and 6 between the measured data and the computed results obtained with the sticking coefficient of 0.85. The computation predicts lower pressures and difference is partially attributed to the use in the simulation of a panel temperature of 40 K instead of the actual value of 15 K. Use of the lower temperature in the simulation is expected to increase the pressure. There is also the requirement to perform a simulation with a cryo-panel sticking coefficient of 0.60 that is at the lower end of the range of values listed in Ref. 19.

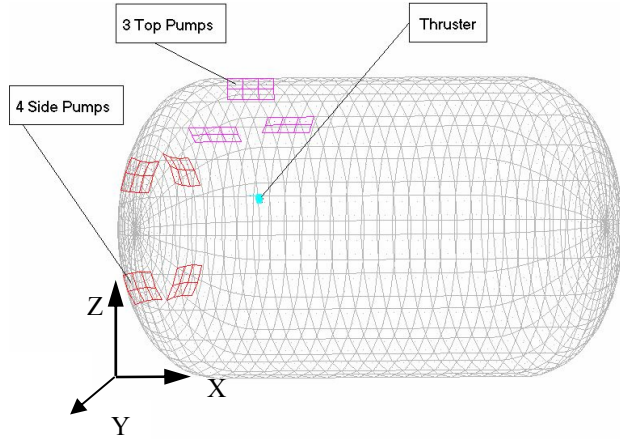


Figure 10 – Computational mesh used in the DSMC computations.

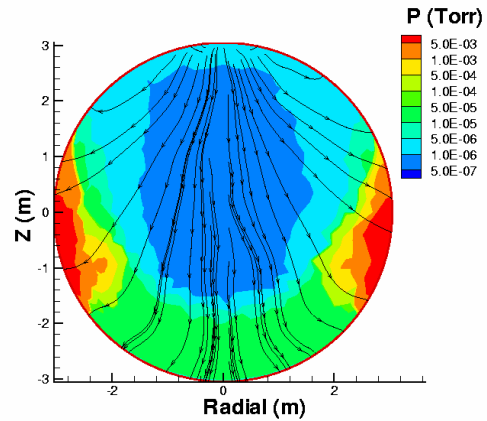


Figure 13 – Contours of pressure predicted by the DSMC computation on the downstream wall of the chamber.

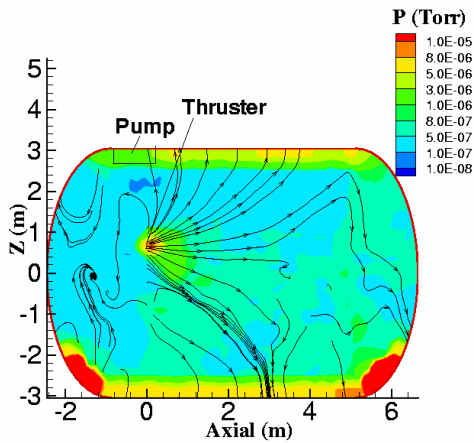


Figure 11 – Contours of pressure predicted by the DSMC computation in the $y=0$, $x-z$ plane.

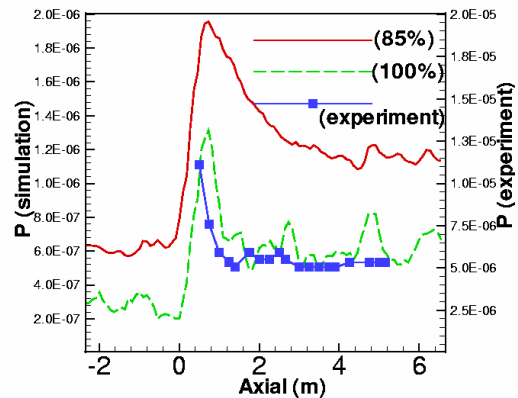


Figure 14 – Profiles of pressure (Torr) in the x -direction along the chamber centerline.

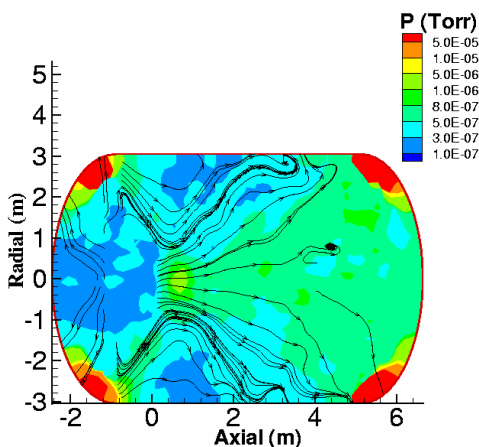


Figure 12 – Contours of pressure predicted by the DSMC computation in the $z=0$, $x-y$ plane.

Conclusions and Future Work

The goal of this work is to create a technique for calibrating a vacuum chamber in terms of pressure to account for elevated back pressures while testing Hall thrusters. A neutral gas background pressure map of the LVTF was created at a series of cold anode flow rates corresponding to P5 Hall thruster operating conditions of 1.5, 3.0, and 9.0 kW. Analysis of the zero anode flowrate maps shows that the current method of estimating chamber background pressure is conservative. The nude ionization gauge gives a better estimate of the true chamber background pressure. Axial pressure profiles on the thruster centerline indicate that the plume expands to the facility background pressure in approximately 1.7 m. The

plume expansion appears to be independent of anode flowrate and facility background pressure. A similar cold-flow mapping will be conducted at NASA GRC in VF-12. A hot flow pressure map of the LVTF will be performed in the near future. The facility background pressure may be of greater importance for the hot flow plume expansion, as CEX collisions will be present.

The experimental results were used to validate the current status of a full 3D-numerical model of the LVTF with a cold flow thruster. The differences between the model and experimental data are attributed to inadequate physical parameters. The literature does not contain the sticking coefficient of xenon onto a cryo-panel. The cryo-panel surface was modeled with a 40 K temperature. The operating temperature of a cyro-panel surface is approximately 13 K. Future numerical work will validate appropriate physical parameters. In addition, model upgrades will include the ability to simulate hot flow.

Acknowledgements

We would like to thank: Robert Jankvosky at NASA Glenn Research Center for his assistance in calibrating the ionization gauges, undergraduate Robert Thomas for his help constructing the IGPS and experimental setup, and the departmental technical staff and other graduate students at PEPL for help in maintaining the facilities. This research was supported by the Air Force Office of Scientific Research grants F49620-00-1-0201 and F49620-01-1-0061 (Dr. Mitat Birkan is the contract monitor for both). The modeling work was supported by the Air Force Research Laboratory with Dr. William Hargus as the technical monitor. In addition, Mr. Mitchell Walker is supported by the Michigan Space Grant Consortium and the National Science Foundation. The authors are greatly appreciative of this support.

References

1. King, L. B., Gallimore, A. D., "Ionic and Neutral Particle Transport Property measurements in the Plume of an SPT-100," 32nd Joint Propulsion Conference, Lake Buena Vista, FL, July 1-3, 1996.
2. Hofer, R. R., Walker, M. L. R., Gallimore, A. D., "A Comparison of nude and collimated Faraday Probes for Use with Hall Thrusters," IEPC-01-20, 27th International Electric Propulsion Conference, Pasadena, CA, Oct 14-19, 2001.
3. Manzella, D. H., Sankovic, J. M., "Hall Thruster Ion Beam Characterization," AIAA-95-2927, 31st Joint Propulsion Conference, San Diego, CA, July 10-12, 1995.
4. Gallimore, A. D., "Near- and Far-Field Characterization of Stationary Plasma Thruster Plumes," Journal of Spacecraft and Rockets, Vol. 38, No. 3, May-June 2001, pp 441-453
5. Semenko, A., Kim, V., Gorshokov, O., Jankovsky, R., "Development of Electric Propulsion Standards – current status and further activity," IEPC-2001-070 27th International Electric Propulsion Conference, Pasadena, Oct. 15-19, 2001.
6. Jankovsky, R. S., Jacobson, D. T., Mason, L. S., Rawlin, V. K., Mantenicks, M. A., Manzella, D. H., Hofer, R. R., Peterson, P. Y., "NASA's Hall Thruster Program," AIAA-2001-3888, 37th Joint Propulsion Conference, Salt Lake City, UT, July 8-11, 2001.
7. Boyd, I. D., "Review of Hall Thruster Plume Modeling," Journal of Spacecraft and Rockets, Vol. 38, No.3, May-June 2001, pp. 381-387
8. Fife, J. M., Hargus, W. Jr, Jaworske, D. A., Sarmient, C., Mason, L., Jankovsky, R., Snyder, J. S., Malone, S., Haas, J., Gallimore, A., "Spacecraft Interaction Test Results of the High Performance Hall System SPT-140," AIAA-2000-3521, 36th Joint Propulsion Conference, Huntsville, AL, July 17-19, 2000.
9. Hofer, R. R., Peterson, P. Y., Gallimore, A. D., "Characterizing Vacuum Facility Backpressure Effects on the Performance of a Hall Thruster," IEPC-01-045, 27th International Electric Propulsion Conference, Pasadena, CA, Oct 14-19, 2001.
10. de Grys, K. H., Tilley, D. L., Aadland, R. S., "BPT Hall Thruster Plume Characteristics," AIAA-99-2283, 35th Joint Propulsion Conference, Los Angeles, CA, June 20-24, 1999.
11. Walker, M. L. R., Hofer, R. R., Gallimore, A. D., "The Effects of Nude Faraday Probe Design on the Measured Ion Current Density Profile of Hall Thruster Plumes," AIAA-2002-4253, 38th Joint Propulsion Conference & Exhibit, Indianapolis, IN, July 7-10, 2002.
12. Dushman, S., *Scientific Foundations of Vacuum Technique*, Vol. 4, Wiley, New York, 1958.
13. Redhead, P. A., "The measurement of vacuum pressures," Journal of Vacuum Science Technology, VA2, No. 2, Apr.-Jun. 1984, pp 132-138
14. Hofer, R. R., Peterson, P. Y., Gallimore, A. D., "A High Specific Impulse Two-Stage Hall Thruster with Plasma Lens Focusing," 27th International

Electric Propulsion Conference, Pasadena, CA, Oct 14-19, 2001.

15. Randolph, T., Kim, V., Kaufman, H., Kozubsky, K., Zhurin, V., Day, M., "Facility Effects on Stationary Plasma Thruster Testing," IEPC-93-93, 23rd International Electric Propulsion Conference, Seattle, WA, Sept 13-16, 1993.
16. Bird, G. A., *Molecular Gas Dynamics and the Direct Simulation of Gas Flows*, Oxford University Press, 1994
17. Dietrich, S. and Boyd, I. D., "Scalar and Parallel Optimized Implementation of the Direct Simulation Monte Carlo Method," *Journal of Computational Physics*, Vol. 126, 1996, pp. 328-342.
18. "HyperMesh 3.0," Altair Engineering Inc., Troy, Michigan, 1994.
19. Ketsdever, A. D., "Design Considerations for Cryogenic Pumping Arrays in Spacecraft-Thruster Interaction Facilities," *Journal of Spacecraft and Rockets*, Vol. 38, No. 3, May-June 2001, pp. 400-410

